CHEMISTRY
A EUROPEAN JOURNAL

DOI: 10.1002/chem.200601865

Redox-Driven Intramolecular Anion Translocation between a Metal Centre and a Hydrogen-Bond-Donating Compartment

Valeria Amendola, Benoît Colasson, Luigi Fabbrizzi,* and Maria-Jesús Rodriguez Douton[a]

Abstract: Dicationic ligands incorporating two 2,2′-bipyridine units and two imidazolium moieties, $[\mathbf{1}]^{2+}$ and $[\mathbf{2}]^{2+}$, form stable chelate complexes with Cu^{II} and Cu^{I} in acetonitrile solution. Each Cu^{II} complex binds two X^- ions according to two stepwise equilibria, the first involving the Cu^{II} centre and the second involving the bis-imidazolium compartment. Cu^{I} complexes are able to host only one NO_3^- ion in the bis-imidazolium cavity, while other anions induce demetallation. Thus, in the presence of one equivalent of NO_3^-, the Cu^{II}/Cu^{I} redox change makes the anion translocate quickly and reversibly from one binding site to the other within the $[Cu^{II,I}(\mathbf{1})]^{4+/3+}$ system, as demonstrated by cyclic voltammetry and controlled-potential electrolysis experiments.

Keywords: anion recognition · copper · hydrogen bonds · molecular machines · redox chemistry

Introduction

The externally controlled motion of a movable part within a supramolecular system provides a way to convert chemical energy into mechanical work at a molecular level and forms the basis of the design of molecular machines. Classical examples include 1) the sliding of the axle of a rotaxane (coupled to either an auxiliary acid–base or redox process)[1] and 2) the half-turn of the ring of a [2]catenate (driven by the Cu^{I}/Cu^{II} redox couple).[2] These have inspired the design of a great number of molecular and supramolecular systems consisting of one movable and one stationary part, whose activity is operated by an input of a chemical, electrochemical or photonic nature.[3] A further type of controlled motion concerns the translocation of an ionic particle between two non-equivalent compartments of a molecular system.[4] Most examples involve the externally driven translocation of transition-metal ions and are based on two distinct protocols: 1) the metal exists in two oxidation states of comparable stability, and oxidation–reduction processes cause its transfer between two compartments of definitely different coordinating tendencies;[5–12] and 2) the coordinating properties of only one compartment towards a given metal ion are altered through an acid–base process, so that consecutive addition of H^+ and OH^- ions induces a reversible intramolecular metal displacement.[13–18] On the other hand, examples of anion translocation are rare and all refer to the redox-driven transfer of an anion between two metal centres within a hetero-dinuclear complex.[19] In particular, the coordinating tendencies of a metal towards a given anion are modified through a one-electron redox change (e.g. Ni^{II}/Ni^{III}), which induces the anion movement to/from a proximate ancillary metal ion (e.g. a coordinatively unsaturated Cu^{II} centre).[20,21]

In recent years, great attention has been devoted to the design of receptors capable of establishing electrostatic and/or hydrogen-bonding interactions with anions, essentially in order to develop optical sensors for anion determination in the biomedical, environmental and food sciences.[22] In particular, guidelines for the synthesis of positively charged or neutral receptors suitable for selective interaction with anions of given size and geometrical features have been outlined.[23] On these bases and in the perspective of setting up further experiments of anion translocation, we considered the design of a ditopic receptor containing a purely organic compartment, capable of establishing hydrogen-bonding in-

[a] Dr. V. Amendola, Dr. B. Colasson,[+] Prof. L. Fabbrizzi, Dr. M.-J. Rodriguez Douton
Dipartimento di Chimica Generale
Università di Pavia
via Taramelli 12, 27100 Pavia (Italy)
Fax: (+39) 0382-528-544
E-mail: luigi.fabbrizzi@unipv.it

[+] Present address:
Laboratoire de Chimie et Biochimie Pharmacologiques et Toxicologiques
Université Paris V
45 Rue des Saints Pères, 75270 Paris Cedex 06 (France)

teractions with anions. The other compartment had to contain a redox-active metal centre in order to provide the engine for the translocation process, which should be fuelled by the energy released by an ancillary oxidation–reduction process.

In particular, we have synthesised the molecular dications $[\mathbf{1}]^{2+}$ and $[\mathbf{2}]^{2+}$, in which two equivalent arms are appended in the 1,4- and 1,3-positions of a phenyl platform, respectively. Each arm contains an imidazolium fragment and a 2,2′-bipyridine subunit. The imidazolium moiety can behave as an H-bond donor, through the polarised C–H fragment between the nitrogen atoms, and is widely used in the design of receptors suitable for multipoint hydrogen-bonding interactions with anions.[24] 2,2′-Bipyridine (bpy) is one of the most classical and investigated ligands in metal coordination chemistry, and forms stable complexes with most transition-metal ions.[25]

We considered that the chelate coordination by the bpy subunits of $[\mathbf{1}]^{2+}$ or $[\mathbf{2}]^{2+}$ of a metal M should generate a closed compartment capable of establishing hydrogen-bonding interactions with a given anion. In particular, H-bonds should be donated to the anion 1) by two C–H fragments from the imidazolium subunits and 2) by the two C–H fragments in the 3-positions of the bpy subunits, which have been activated through the coordination of bpy to the metal.[26] Then, we thought that the redox couple Cu^{II}/Cu^{I} could work as an effective switch for anion translocation. In fact, the model complex $[Cu^{II}(bpy)_2]^{2+}$ tends to bind an anion X^- to give the solution-stable five-coordinate ternary species $[Cu^{II}(bpy)_2(X)]^+$, whose coordination polyhedron is a trigonal bipyramid, slightly distorted towards the square pyramid.[27] Thus, in a solution containing equimolar amounts of $[Cu^{II}(L)]^{4+}$ ($[L]^{2+}=[\mathbf{1}]^{2+}$ or $[\mathbf{2}]^{2+}$) and of a selected X^- ion, the anion should be bound to the metal centre to give the $[Cu^{II}(L)(\leftarrow X)]^{3+}$ complex (the arrow denotes the metal–anion coordinative bond). On one-electron reduction of $[Cu^{II}(L)(\leftarrow X)]^{3+}$, the Cu^{I} centre forms, which exhibits a definite preference towards four-coordination by the two bpy molecules, according to a flattened tetrahedral arrangement.[28] Under these conditions, the X^- anion will be extruded from the coordination sphere of the metal and will move to the close H-bond-donating compartment, to give the translational isomer $[Cu^{I}(L)(\cdots X)]^{2+}$ (the (···) symbol indicating the hydrogen-bonding interaction within the imidazolium compartment). The hypothesised translocation process for $[L]^{2+}=[\mathbf{1}]^{2+}$ is depicted in Scheme 1.

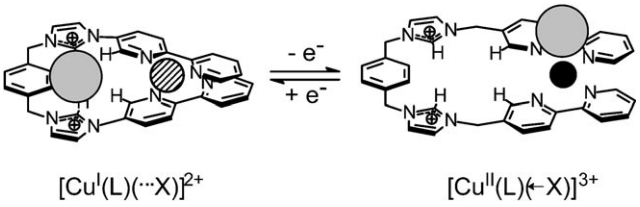

Scheme 1. The planned translocation of an anion X^- (grey sphere) within the $[Cu^{II,I}(\mathbf{1})]^{4+/3+}$ system, driven by the Cu^{II}/Cu^{I} redox couple (Cu^{I}: hashed sphere; Cu^{II}: black sphere). The redox change induces a change of the coordination geometry at the metal centre, from tetrahedral (Cu^{I}) to a five-coordinate arrangement (Cu^{II}, square pyramidal or trigonal bipyramidal).

It should be noted that the positive electrical charge of the two complexes $[Cu^{I}(L)(\cdots X)]^{2+}$ and $[Cu^{II}(L)(\leftarrow X)]^{3+}$ is neutralised by two and three Y^- counterions (PF_6^-, $CF_3SO_3^-$, ClO_4^-), respectively, which are dispersed in the acetonitrile (MeCN) solution and do not participate in the translocation process. In particular, PF_6^-, $CF_3SO_3^-$ and ClO_4^- have been chosen as counterions in view of their poor or zero tendencies to coordinate metal centres and to establish hydrogen-bonding interactions.

The success of the translocation experiment illustrated above requires the fulfilment of several conditions: 1) system $[L]^{2+}$ should be able to form stable chelate complexes with both Cu^{I} and Cu^{II}; the issue is not marginal, as metal chelation could be contrasted with the electrostatic repulsion by the facing imidazolium subunits; 2) in the $[Cu^{II}(L)(X)]^{3+}$ complex, the X^- ion should exhibit a definitely higher affinity for the metal than for the imidazolium compartment; and 3) the envisioned X^- ion should not compete with bpy for the metal, either Cu^{I} or Cu^{II}.

In this work, detailed equilibrium studies have been carried out in MeCN solution on the interaction of $[\mathbf{1}]^{2+}$ and $[\mathbf{2}]^{2+}$ with Cu^{II} and Cu^{I}, and on the association of the corresponding complexes with a variety of inorganic anions, to define the conditions for the occurrence of the anion translocation process. It is anticipated that a reversible, electrochemically driven translocation between the two compartments of the $[Cu^{II,I}(\mathbf{1})]^{4+/3+}$ system occurs with the nitrate ion.

Results and Discussion

The formation of $[Cu^{II}(\mathbf{1})]^{4+}$ and $[Cu^{II}(\mathbf{2})]^{4+}$ complexes and their interactions with anions: The complexation of Cu^{II} by $[\mathbf{1}]^{2+}$ and $[\mathbf{2}]^{2+}$ was investigated by titrating a solution of $[\mathbf{1}](PF_6)_2$ in MeCN (3.70×10^{-4} M) with a standard solution of $Cu^{II}(CF_3SO_3)_2$ in MeCN. PF_6^- and $CF_3SO_3^-$ were chosen as counter anions in view of their very poor or zero coordinating tendencies towards metal ions.

Figure 1a shows the spectra taken over the course of the titration of $[\mathbf{1}]^{2+}$. Cu^{II} binding is demonstrated by the dramatic modifications observed in the UV spectral region. In

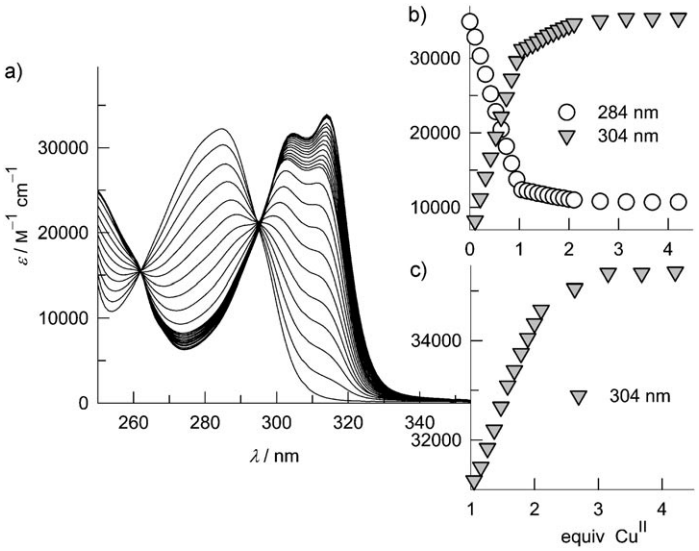

Figure 1. a) UV spectra recorded over the course of the titration of a solution of $[\mathbf{1}]^{2+}$ in MeCN (3.7×10^{-4} M) with a standard solution of $Cu^{II}(CF_3SO_3)_2$ in MeCN; b) titration profiles at 284 (○) and 304 nm (▼); and c) titration profile at 304 nm, after addition of one equivalent of Cu^{II}.

particular, on Cu^{II} addition the intensity of the band centred at 284 nm, which arises from π–π* transitions in the bpy subunits, decreases, while a new band, split into two distinct transitions centred at 304 and 316 nm, forms and develops. These spectral changes may result from the alteration of the π energy levels of the bpy moiety, following their interaction with the dπ orbitals of Cu^{II}. In any case, the course of the metal complexation is unambiguously illustrated by titration profiles at selected wavelengths. As an example, Figure 1b shows the variation of the absorbance at 284 and 304 nm, induced by Cu^{II} addition. The sharp decrease (284 nm)/increase (304 nm) of the absorbances observed on addition of the first equivalent of Cu^{II} is indicative of the formation of a rather stable $[Cu^{II}(\mathbf{1})]^{4+}$ complex, according to the equilibria [Eqs. (1) and (2)]:

$$Cu^{2+} + [\mathbf{1}]^{2+} \rightleftharpoons [Cu^{II}(\mathbf{1})]^{4+} \quad (1)$$

$$[Cu^{I}(\mathbf{1})]^{4+} + Cu^{2+} \rightleftharpoons [Cu_2{}^{II}(\mathbf{1})]^{6+} \quad (2)$$

In the $[Cu^{II}(\mathbf{1})]^{4+}$ species, the Cu^{II} centre should be coordinated by the two bpy subunits of $[\mathbf{1}]^{2+}$. An MeCN molecule may complete the five-coordinate geometrical arrangement preferred by the Cu^{II} centre. After the addition of one equivalent of Cu^{II}, a neat slope change is observed, which corresponds to the formation of the $[Cu_2{}^{II}(\mathbf{1})]^{6+}$ dimetallic species, according to the stepwise equilibrium (2). In this species, the ligand $[\mathbf{1}]^{2+}$ has opened its arms, so that each bpy subunit can coordinate one Cu^{II} ion. The steep titration profile over the 0–1 equivalent interval prevented any safe determination of the complexation constants K_{1M}, whose value can only be estimated as $>10^6$. In any case, the fact that $\log K_{1M} > 6$ allows one to assume that, in the concentration scale used in the studies described below ($\geq 10^{-4}$ M) and in a solution equimolar in both **1** and $Cu^{II}(CF_3SO_3)_2$, the $[Cu^{II}(\mathbf{1})]^{4+}$ complex is the highly dominant metal-containing species present (>99%). On the other hand, the profile observed after the addition of one equivalent (see Figure 1c) shows a curvature suitable for a safe determination of the pertinent equilibrium constant. In particular, on processing the titration data by a non-linear least-squares procedure,[29] a $\log K_{2M}$ value of 4.4 ± 0.1 was calculated. A similar spectral pattern was obtained on titration with Cu^{II} of a solution of $[\mathbf{2}]^{2+}$ in MeCN, and the formation of a very stable $[Cu^{II}(\mathbf{2})]^{4+}$ complex could be ascertained ($\log K_{1M} > 6$; $\log K_{2M} = 3.3\pm0.1$).

To study the interaction of the $[Cu^{II}(\mathbf{1})]^{4+}$ receptor with anions, a solution of $[\mathbf{1}]^{2+}$ and $Cu^{II}(CF_3SO_3)_2$ in MeCN (both 10^{-4} M) was prepared and titrated with a standard solution of a $[Bu_4N]X$ salt in MeCN. Figure 2a shows the family of spectra taken in the visible region over the course of the titration of a solution of $[Cu^{II}(\mathbf{1})]^{4+}$ (1.01×10^{-4} M) with $[Bu_4N]Br$.

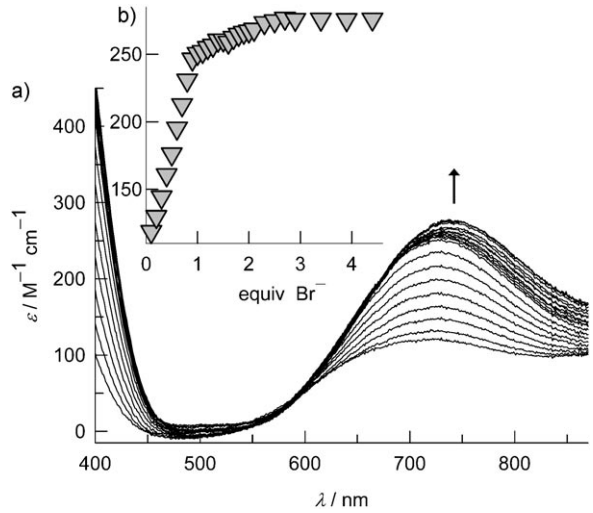

Figure 2. a) Spectra recorded in the visible region over the course of the titration of a solution of $[Cu^{II}(\mathbf{1})]^{4+}$ in MeCN (1.01×10^{-4} M) with a standard solution of $[Bu_4N]Br$ in MeCN. Optical path: 1 cm; ε: molar absorbance. b) Titration profile at 745 nm.

Attention is focussed on the region of d–d transitions. In particular, before Br^- addition, a broad band centred at approximately 700 nm is observed. Such a band should be the envelope of the d–d transitions occurring in the five-coordinate $[Cu^{II}(N\hat{}N)_2(MeCN)]^{2+}$ complex, where N^N indicates each bpy fragment of **1**. On Br^- addition, the band is red-shifted, while its intensity progressively increases. Such a spectral change has to be ascribed to the replacement of the coordinated MeCN molecule by a bromide ion, to give the

$[Cu^{II}(N^{\wedge}N)_2(Br)]^+$ ternary complex. The titration profile in Figure 2b shows an abrupt slope change on addition of one equivalent of Br^-, indicating that the formation equilibrium of the $[Cu^{II}(\mathbf{1})(Br)]^{3+}$ species is characterised by a constant K_1 whose value is higher than 10^6. On further addition of bromide, minor spectral changes are observed, as emphasised by the very moderate slope of the titration profile over the interval of 1–2 equivalents of Br^-. It is tentatively suggested that such small changes can be ascribed to a rearrangement of the five-coordinate copper complex, induced by the binding of a second Br^- ion by the bis-imidazolium compartment. However, more direct evidence on the occurrence of this second equilibrium could be obtained from spectra recorded in the UV region (see Figure 3a).

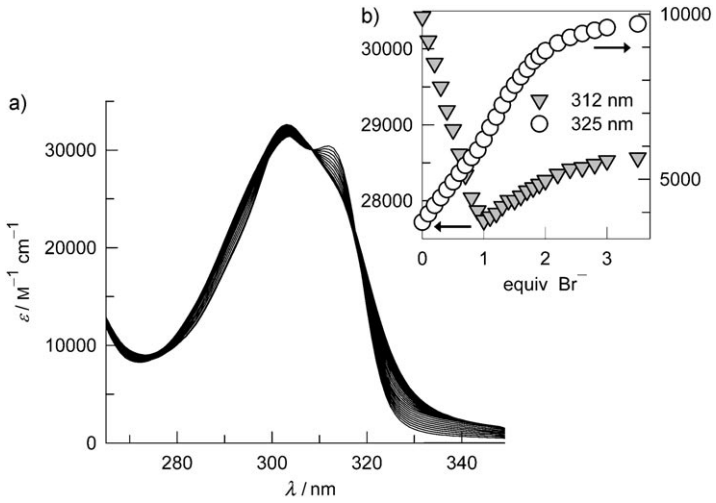

Figure 3. a) Spectra recorded in the UV region over the course of the titration of a solution of $[Cu^{II}(\mathbf{1})]^{4+}$ in MeCN (1.01×10^{-4} M) with a standard solution of $[Bu_4N]Br$ in MeCN. Optical path: 0.1 cm. b) Titration profiles at 312 nm (▼, left vertical axis) and at 325 nm (○, right vertical axis).

In particular, subtle but significant spectral modifications are observed over the course of the titration. For instance, the band centred at 312 nm decreases steeply during the addition of the first equivalent of Br^- (see the titration profile, triangles, in Figure 3b). However, after the addition of one equivalent, the absorbance stops decreasing and increases with a smooth curvature, which indicates the occurrence of two distinct and consecutive processes. It is suggested that in the 0–1 equivalent interval, the Br^- ion goes to bind the metal and forms the $[Cu^{II}(N^{\wedge}N)_2(Br)]^+$ ternary complex. The charge density transferred on the metal affects indirectly, but significantly, the π–π* transition within the bpy subunit responsible for the band at 312 nm, whose intensity abruptly decreases. It is then assumed that the second Br^- ion goes to interact with the bis-imidazolium compartment: this process still has an effect on the π–π* transition within the bpy subunit, but it operates in the opposite direction, inducing an increase of the absorbance. The interference of the second Br^- ion with the electronic transitions of the bpy subunits can be explained by assuming that Br^- accepts H-bonds not only from the C–H_α fragments of the imidazolium subunits, but also from the C–H_β fragments of the close pyridine rings, which have been polarised through the coordination of the bpy subunits to the Cu^{II} centre. Noticeably, the establishing of a definite hydrogen-bonding interaction between the bromide ion and the C–H_β fragments in an Fe^{II}-containing bpy–imidazolium cage has been recently demonstrated through crystallographic and ^1H NMR spectroscopic results.[26] Discontinuity in spectral effects induced by anion addition is observed in any portion of the spectra. For instance, the profile of the absorbance at 325 nm (circles in Figure 3b) shows a definite change of slope after the addition of one equivalent of Br^-. Also in this case, the steepness of the 0–1 equivalent segment prevents the determination of K_1, whose value should be higher than 10^6. On the other hand, the smooth profile observed after one equivalent would allow the determination of a binding constant. In particular, on multi-wavelength treatment of titration data through a non-linear least-squares procedure,[29] a value of $\log K_2 = 4.62 \pm 0.06$ was calculated. Thus, the interaction of the $[Cu^{II}(\mathbf{1})]^{4+}$ receptor with the Br^- ion can be described through the stepwise equilibria (3) and (4), which give the receptor–anion complexes $[Cu^{II}(\mathbf{1})(\leftarrow Br)]^{3+}$ and $[Cu^{II}(\mathbf{1})(\leftarrow Br)(\cdots Br)]^{2+}$.

$$[Cu^{II}(\mathbf{1})]^{4+} + Br^- \rightleftharpoons [Cu^{II}(\mathbf{1})(\leftarrow Br)]^{3+} \quad (3)$$

$$[Cu^{II}(\mathbf{1})(\leftarrow Br)]^{3+} + Br^- \rightleftharpoons [Cu^{II}(\mathbf{1})(\leftarrow Br)(\cdots Br)]^{2+} \quad (4)$$

The occurrence of two distinct consecutive equilibria was also ascertained for the anions Cl^-, NCS^-, and NO_3^- through analogous titration experiments: the corresponding log$K$ values are reported in Table 1.

Table 1. Log$K$ values for anion complexation equilibria in MeCN solution at 25 °C. In parentheses: the standard deviation on the last figure.

Equilibrium		Cl^-	Br^-	NCS^-	NO_3^-
$[Cu^{II}(\mathbf{1})]^{4+}+X^-$	$\log K_1$	>6	>6	>6	5.35(4)
$[Cu^{II}(\mathbf{1})\leftarrow X]^{3+}+X^-$	$\log K_2$	5.20(8)	4.62(6)	3.62(3)	3.49(4)
$[Cu^{I}(\mathbf{1})]^{3+}+X^-$	$\log K$	–[a]	–[a]	–[a]	3.29(1)
$[Cu^{II}(\mathbf{2})]^{4+}+X^-$	$\log K_1$	>6	>6	>6	5.53(4)
$[Cu^{II}(\mathbf{2})\leftarrow X]^{3+}+X^-$	$\log K_2$	5.03(9)	4.31(9)	3.41(9)	3.69(4)
$[Cu^{I}(\mathbf{2})]^{3+}+X^-$	$\log K_2$	–[a]	–[a]	–[a]	3.56(1)

[a] The anion demetallates the receptor.

Whereas for the strongly coordinating anions Cl^- and NCS^- $\log K_1$ values >6 were estimated, in the case of NO_3^- a definite value of the first binding constant could be determined ($\log K_1 = 5.35 \pm 0.04$). On the other hand, $\log K_2$ values were observed to decrease according to the sequence: $Cl^- > Br^- > NCS^- \approx NO_3^-$, which reflects the decrease of the H-bond acceptor tendencies of the anion. Titration with $[Bu_4N]I$ resulted in oxidation to I_3^-. Addition of HSO_4^- and $H_2PO_4^-$ induced precipitation.

The same behaviour was observed for the isomeric system $[\mathbf{2}]^{2+}$, that is, a stable $[Cu^{II}(\mathbf{2})]^{4+}$ complex formed, which behaved as an anion receptor for Cl^-, Br^-, NCS^- and NO_3^-. The $\log K_1$ and $\log K_2$ values, reported in Table 1, are quite similar to those observed for the $[Cu^{II}(\mathbf{1})]^{4+}$ receptor. Thus, it is concluded that appending the two imidazolium–bpy arms, whether in the 1,4- or 1,3-position of the phenyl platform, neither significantly modifies the coordination geometry and the binding tendencies of the $[Cu^{II}(L)_2]^{2+}$ subunit (K_1) nor alters the spatial arrangement and the H-bond-donating properties of the imidazolium compartment (K_2).

The formation of $[Cu^{I}(1)]^{3+}$ and $[Cu^{I}(2)]^{3+}$ complexes and their interactions with anions: The complexation of Cu^I by $[\mathbf{1}]^{2+}$ and $[\mathbf{2}]^{2+}$ in MeCN was first investigated by titrating a solution of the ligand with a standard solution of $[Cu^I(MeCN)_4]ClO_4$. The interaction of the Cu^I ion with the bpy subunits of $[\mathbf{1}]^{2+}$ and $[\mathbf{2}]^{2+}$ could be visually perceived, even in a diluted solution, through the appearance of a brick-red colour, which is ascribed to a rather intense absorption band centred at 450 nm of metal-to-ligand charge-transfer (MLCT) nature. The development of such a band in the case of system $[\mathbf{1}]^{2+}$ is illustrated in Figure 4a, while the titration profile at 456 nm is shown in Figure 4b. The slope change observed in the profile at one equivalent of added Cu^I suggests the occurrence of two consecutive equilibria involving: 1) the formation of the $[Cu^I(\mathbf{1})]^{3+}$ complex, in which the metal centre is coordinated by the two bpy subunits of $[\mathbf{1}]^{2+}$ over the 0–1 equivalent interval, and 2) the formation of the dimetallic complex $[Cu_2^I(\mathbf{1})]^{4+}$, in which each bpy subunit of $[\mathbf{1}]^{2+}$ binds a copper(I) centre.

In particular, the best-fitting of titration data over the 200–600 nm spectral range was observed on assuming the occurrence of the two equilibria (5) and (6), whose constants are: $\log\beta_1 = \log K_{1M} = 4.26 \pm 0.01$ and $\log\beta_2 = 6.58 \pm 0.05$.

$$Cu^+ + [\mathbf{1}]^{2+} \rightleftharpoons [Cu^I(\mathbf{1})]^{3+} \quad (5)$$

$$2\,Cu^+ + [\mathbf{1}]^{2+} \rightleftharpoons [Cu_2^I(\mathbf{1})]^{4+} \quad (6)$$

$$[Cu^I(\mathbf{1})]^{3+} + Cu^+ + \rightleftharpoons [Cu_2^I(\mathbf{1})]^{4+} \quad (7)$$

Notice that the constant referring to the stepwise equilibrium (7), $\log K_{2M}$, can be obtained from the difference $(\log\beta_2 - \log\beta_1) = 2.32 \pm 0.06$. The interaction of Cu^I with $[\mathbf{1}]^{2+}$ could also be followed by investigating the spectral changes in the UV region (Figure 4c). In particular, on Cu^I binding, the band centred at 280 nm, originating from π–π^* transitions within the bpy subunits, is split into two bands centred at 265 and 300 nm.

Figure 5a shows the percentage concentration of the species present at the equilibrium over the course of the titration experiment illustrated in Figure 4. It is observed that the dimetallic species $[Cu_2^I(\mathbf{1})]^{4+}$ is formed in an appreciable amount only on addition of a substantial excess of Cu^I (13% at 5 equiv). In any case, the formation of such a dimetallic species must be assumed to ensure a fully satisfactory fitting of titration data over the entire titration range.

The interaction of the Cu^I ion with ligand $[\mathbf{1}]^{2+}$ was also investigated by titrating a solution of $[Cu^I(MeCN)_4]ClO_4$ in MeCN with a standard solution of $[\mathbf{1}](PF_6)_2$ (i.e. in the opposite way with respect to the titration experiment illustrated in Figure 4).

Figure 6a shows the visible portion of the spectra taken over the course of the titration, while Figure 5b displays the titration profile at 450 nm. Best-fitting of titration data was achieved by assuming the occurrence of equilibria (5) and (6), to which the following constants corresponded: $\log\beta_1 = 4.23 \pm 0.01$ and $\log\beta_2 = 6.7 \pm 0.1$. The values are in good agreement with those obtained from the titration experiments illustrated in Figure 4 (metal added to the ligand). Figure 5b shows the percentage concentration of the species present at the equilibrium over the course of the titration experiments. It is observed that the dimetallic species $[Cu_2^I(\mathbf{1})]^{4+}$ is formed in a very small amount (the maximum concentration of about 1% being achieved on addition

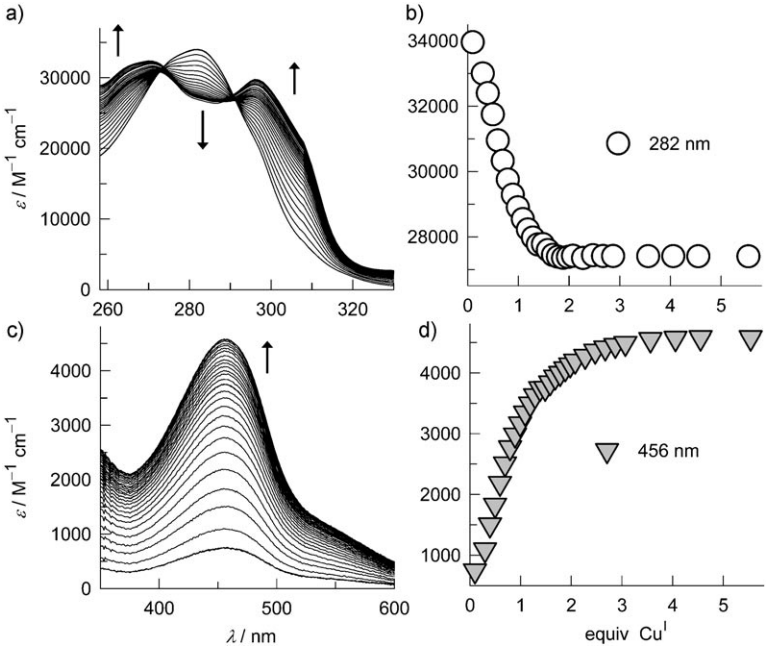

Figure 4. Spectra recorded over the course of the spectrophotometric titration of a solution of $[\mathbf{1}](PF_6)_2$ in MeCN (3.9×10^{-4} M) with a standard solution of $[Cu^I(MeCN)_4]ClO_4$ in MeCN; a) visible portion (MLCT transitions); c) UV portion (π–π^* transitions within the bpy subunits); b,d) titration profiles at selected wavelengths.

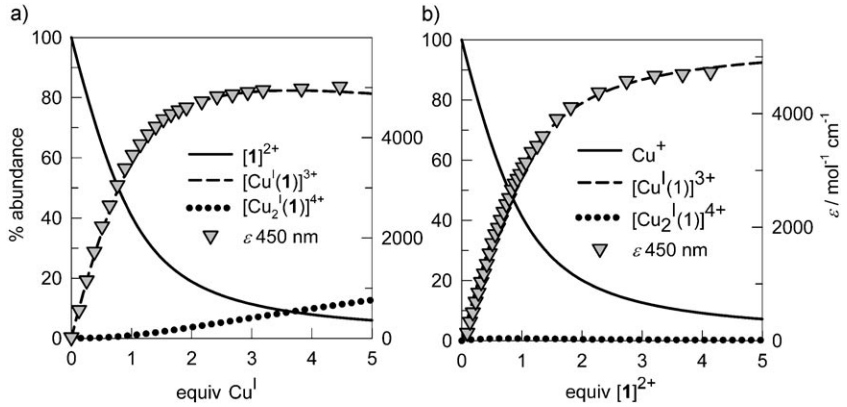

Figure 5. Percentage concentrations (——, left vertical axis) and molar absorbance at 450 nm (▼, right vertical axis) pertinent to titrations of a) a solution of $[\mathbf{1}](PF_6)_2$ in MeCN with a standard solution of $[Cu^I(MeCN)_4]ClO_4$; and (b) a solution of $[Cu^I(MeCN)_4]ClO_4$ in MeCN with a standard solution of $[\mathbf{1}](PF_6)_2$ in MeCN.

in most cases the decomposition of the $[Cu^I(\mathbf{1})]^{3+}$ complex, as inferred by a decrease of the intensity of the MLCT band and the disappearance of the brick-red colour since the first additions of the tetraalkylammonium salt.

As an example, Figure 7a shows the spectra taken over the course of the titration with $[Bu_4N]NCS$. The band pertinent to the MLCT transition in the Cu^I–polypyridine complex progressively decreases on anion addition, as also indicated by the absorbance profile in Figure 7b.

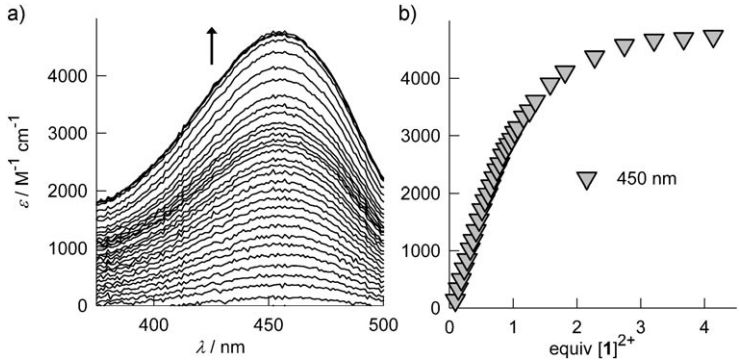

Figure 6. Spectra recorded over the course of the spectrophotometric titration of a solution of $[Cu^I(MeCN)_4]ClO_4$ in MeCN (2.00×10^{-4} M) with a standard solution of $[\mathbf{1}](PF_6)_2$ in MeCN; a) visible portion (MLCT transitions) and b) titration profile at 450 nm.

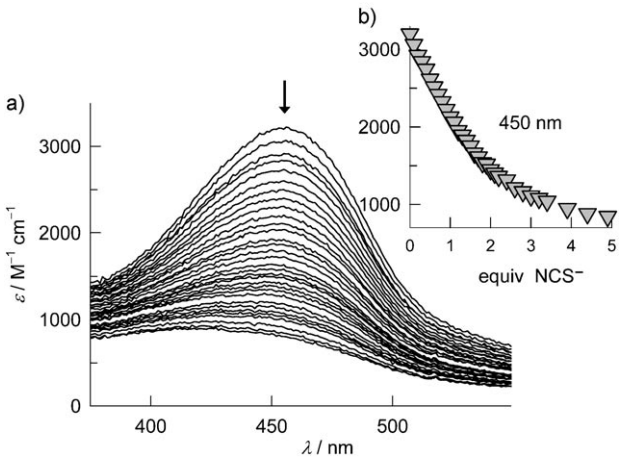

Figure 7. a) Spectra recorded over the course of the spectrophotometric titration of a solution of $[\mathbf{1}](PF_6)_2$ and $[Cu^I(MeCN)_4]ClO_4$ in MeCN (both 3.00×10^{-4} M) with a standard solution of $[Bu_4N]NCS$ in MeCN. b) Titration profile at 450 nm.

of 0.8–1.0 equiv of $[\mathbf{1}]^{2+}$). In any case, it has to be noted that the presence of the dimetallic complex $[Cu_2^I(\mathbf{1})]^{4+}$ is not strictly relevant for data fitting. Quite interestingly, for both titration experiments the absorbances of the MLCT band superimpose well on the concentration of the $[Cu^I(\mathbf{1})]^{3+}$ complex (see triangles in Figure 5a and b).

The higher stability of the $[Cu^{II}(\mathbf{1})]^{4+}$ complex ($\log\beta_1 > 6$) with respect to the monovalent species $[Cu^I(\mathbf{1})]^{3+}$ ($\log\beta_1 = 4.2$) is not surprising and reflects 1) the crystal-field stabilisation effects experienced by the Cu^{II} (d^9) and not by Cu^I (d^{10}), 2) the higher coordination number n of the Cu^{II} complex ($n=5$: 2 N^N + 1 MeCN) with respect to Cu^I ($n=4$, no solvent molecules in the coordination sphere; the comparison is fair, as both uncomplexed Cu^{II} and Cu^I are present in solution as tetra-solvated cations).

Then, the capability of the $[Cu^I(\mathbf{1})]^{3+}$ complex to act as an anion receptor was investigated by titrating a solution of $[\mathbf{1}](PF_6)_2$ and $[Cu^I(MeCN)_4]ClO_4$ in MeCN (both 3.00×10^{-4} M) with a solution of the chosen $[Bu_4N]X$ salt. Experiments were frustrating with most anions, as anion addition induced

Notice that a totally similar behaviour was also observed on addition of NCS^- to an MeCN solution of the model complex $[Cu^I(bpy)_2]^+$. In particular, Cu^I–polypyridine complexes in a MeCN solution are unstable with respect to the a addition of X^- anions, which form the more stable $[Cu^IX_4]^{3-}$ complexes. In this connection, one would expect that $[Cu^I(\mathbf{1})]^{3+}$ species should display extra stability due to the chelate effect. However, it is suggested that such an additional stability is cancelled by the electrostatic repulsions exerted by the two facing imidazolium subunits within the chelate complex.

Quite happily, on titration with NO_3^-, the MLCT band remained intact and colour did not disappear even after addition of a large excess of anion. On the other hand, significant spectral modifications were observed in the π–π^* region, as shown in Figure 8a.

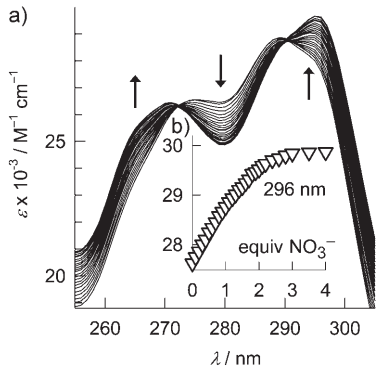

Figure 8. a) Spectra recorded in the UV region over the course of the titration of a solution of $[Cu^I(\mathbf{1})]^{3+}$ in MeCN (3.01×10^{-4} M) with a standard solution of $[Bu_4N]NO_3$ in MeCN. b) Titration profile at 296 nm.

Figure 8b shows the titration profile at a selected wavelength. Best-fitting of spectral data was obtained on assuming the formation of a 1:1 receptor/anion adduct, according to Equation (8):

$$[Cu^I(\mathbf{1})]^{3+} + NO_3^- \rightleftharpoons [Cu^I(\mathbf{1})(\cdots NO_3)]^{2+} \quad (8)$$

with an association constant $\log K = 3.29 \pm 0.01$. It is suggested that, in this complex, nitrate establishes hydrogen-bonding interactions with the bis-imidazolium compartment. In particular, the NO_3^- ion should interact not only with imidazolium C–H_α fragments, but also with the C–H_β fragments of metal-bound bpy subunits, which explains the effect on the π–π* transitions centred on the bpy moieties. The occurrence of hydrogen-bonding interactions at the bis-imidazolium compartment is indirectly demonstrated by the fact that, on titration of the $[Cu^I(Mebpy)_2]^+$ (Mebpy: 5-methyl-2,2′-bipyridine) model system with nitrate, no spectral modifications were observed in either the UV or the visible regions.

The $[\mathbf{2}]^{2+}$ system exhibited a similar behaviour, as far as the complexation equilibria (5) and (6) are concerned ($\log\beta_1 = 4.55 \pm 0.02$, $\log\beta_2 = 7.27 \pm 0.05$, determined from the metal-added-to-ligand procedure). Then, a $\log K = 3.56 \pm 0.01$ was determined for the nitrate-association equilibrium (7).

These studies suggest that translocation experiments could be carried out by operating on a solution containing equimolar amounts of NO_3^- and of the copper–L system. When copper is in the +2 oxidation state, the anion should be bound to the metal centre. Electrochemical reduction to Cu^I should make the anion translocate to the proximate bis-imidazolium compartment. Then, the NO_3^- ion could be relocated at will in one of the two sites by switching the potential of the working electrode between two definite values, in electrochemical experiments that are both dynamic (cyclic voltammetry, CV) and static (controlled-potential electrolysis).

Electrochemically driven nitrate translocation: The occurrence of the redox-controlled NO_3^- translocation process was first investigated through CV experiments. For comparative purposes, the redox behaviour of the model system $[Cu^{II,I}(Mebpy)_2]^{2+/+}$ was preliminarily investigated.

Figure 9a shows the CV profile obtained at a platinum working electrode on a solution of $[Cu^{II}(Mebpy)_2](ClO_4)_2$ in MeCN (2.00×10^{-3} M; dashed line). The process is poorly reversible ($\Delta p = 150$ mV at a potential scan rate of 500 mV s^{-1}), due to the high kinetic barrier associated with the change of the coordination geometry of the redox-active

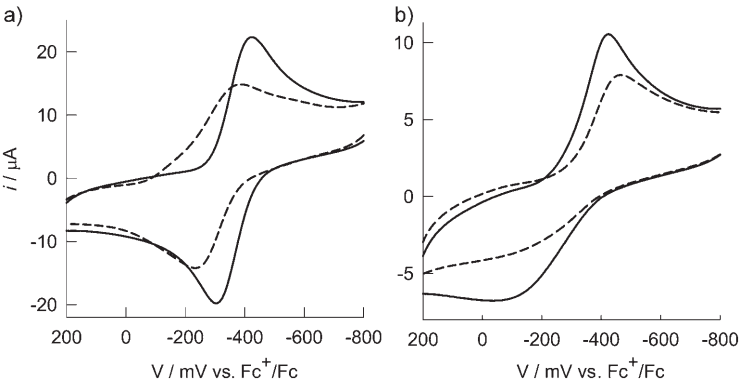

Figure 9. CV profiles obtained at the platinum working electrode (potential scan rate 500 mV s^{-1}) in a solution of $[Bu_4N]ClO_4$ in MeCN (0.1 M). a) (-----) $[Cu^{II}(Mebpy)_2]^{2+}$ (2.00×10^{-3} M), (——) + excess $[Bu_4N]NO_3$; b) (-----) $[\mathbf{1}]^{2+}$ and $Cu^{II}(CF_3SO_3)_2$ (both 1.5×10^{-3} M); (——) + $[Bu_4N]NO_3$ (1.0 equiv).

metal centre: from distorted tetrahedral of Cu^I to distorted trigonal-bipyramidal of Cu^{II}. On titration with nitrate, the CV profile became more reversible ($\Delta p = 120$ mV) and both reduction and oxidation peaks were shifted towards more negative potentials. The solid line in Figure 9a refers to the CV profile taken in the presence of a large excess of $[Bu_4N]NO_3$; its $E_{1/2}$ value is 55 mV more negative than that recorded in the absence of NO_3^-. The anion-induced increase of electrochemical reversibility can be tentatively ascribed to a beneficial involvement of NO_3^- in the activated complex that forms during the change of the coordination geometry. On the other hand, the cathodic shift of the potential simply reflects the thermodynamic stabilisation of the Cu^{II} complex, which takes advantage from the coordination of NO_3^- (which replaces a coordinated MeCN molecule). Needless to say, the coordinatively saturated Cu^I complex cannot profit from such an effect.

Figure 9b displays the CV profile of a solution containing equimolar amounts of $[\mathbf{1}]^{2+}$ and $Cu^{II}(CF_3SO_3)_2$ (dashed line). It is observed that the electrochemical reversibility is lower than that observed in the model system $[Cu^{II,I}(Mebpy)_2]^{2+/+}$ ($\Delta p \approx 400$ mv at 500 mV s^{-1}): the geometrical rearrangement associated with the Cu^I-to-Cu^{II} change involves a substantial change of the angle between the planes containing the bpy subunits. It is possible that, in the course

of the $[Cu^{II,I}(\mathbf{1})]^{4+/3+}$ redox change, such a rearrangement is made sterically difficult by the presence of the carbon chain linking the two bpy moieties. Addition of one equivalent of NO_3^- renders the CV profile more reversible ($\Delta p \approx 300$ mV) and, most interestingly, makes the cathodic peak (associated with the Cu^{II}-to-Cu^{I} reduction) less negative, an opposite behaviour with respect to what is seen with the $[Cu^{II,I}(Mebpy)_2]^{2+/+}$ system. The observed stabilisation of the $[Cu^{I}(\mathbf{1})]^{3+}$ form can be ascribed to the fact that, on Cu^{II}/Cu^{I} reduction, the leaving NO_3^- ion does not move to the bulk solution but goes to the close bis-imidazolium compartment, thus profiting from a favourable energy term not experienced by the reference system $[Cu^{I}(Mebpy)_2]^+$. Thus, in the voltammetric cycles, NO_3^- moves back and forth, quickly and reversibly, between the metal centre and H-bond-donating cavity.

The occurrence of the translocation process was characterised under bulk conditions in a controlled-potential electrolysis experiment. The electrolytic cell, equipped with a working electrode (platinum gauze), a counter-electrode (platinum coil) and a reference electrode (platinum wire, internally calibrated through the Fc^+/Fc couple; Fc: ferrocene), contained a solution of $[\mathbf{1}]^{2+}$, $Cu^{II}(CF_3SO_3)_2$ and $[Bu_4N]NO_3$ in MeCN (all 4.00×10^{-3} M). Under these conditions, it is calculated that the $[Cu^{II}(\mathbf{1})(\leftarrow NO_3)]^{3+}$ species is present at 81% (with respect to the total Cu). The spectrum of this solution is shown in Figure 10a (black solid line). Then, the potential of the platinum gauze was set at -700 mV versus Fc^+/Fc. The consumption of one equivalent of electrons was ascertained through coulometry, while the solution took on a brick-red colour. The spectrum of the electrolysed solution, shown in Figure 10a (solid grey line), is that previously observed in the formation of the $[Cu^{I}(\mathbf{1})(\cdots NO_3)]^{2+}$ complex (see Figure 5a). The calculated percentage concentration of this complex, under the conditions of the electrolysis experiment, is 77%. On setting the potential of the working electrode at 100 mV versus Fc^+/Fc, the solution decolourises and the spectrum of the $[Cu^{II}(\mathbf{1})(\leftarrow NO_3)]^{3+}$ complex is restored (dashed black line in Figure 10a). Then, on exhaustive reduction at -700 mV, the spectrum of the $[Cu^{I}(\mathbf{1})(\cdots NO_3)]^{2+}$ species forms again (dashed grey line in Figure 10a), without any substantial decomposition. The switching nature of the process is illustrated in Figure 10b, which reports the absorbance at 295 nm after the completion of every electrolytic cycle.

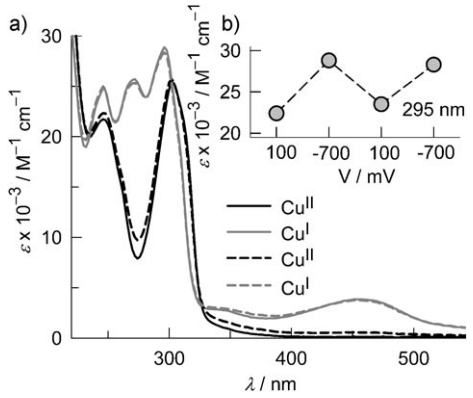

Figure 10. a) Spectra recorded after a cycle of exhaustive electrolysis experiments on a solution of $[Bu_4N]ClO_4$ (0.1 M), $[\mathbf{1}]^{2+}$ (4.00×10^{-3} M), $Cu^{II}(CF_3SO_3)_2$ (4.00×10^{-3} M) and $[Bu_4N]NO_3$ (4.00×10^{-3} M) in MeCN. Optical path: 0.01 cm. Spectral changes accompany the translocation of the NO_3^- anion, according to the redox equilibrium: $[Cu^{II}(\mathbf{1})(\leftarrow NO_3)]^{3+} + e^- \rightleftharpoons [Cu^{I}(\mathbf{1})(\cdots NO_3)]^{2+}$; b) absorbance at 295 nm, after the completion of every electrolytic cycle.

While the occurrence of a reversible translocation of a NO_3^- ion from the Cu^{II} metal centre to the bis-imidazolium compartment of the $[Cu^{I}(\mathbf{1})]^{3+}$ system has been demonstrated (in a process involving about 80% of the copper complexes in solution, at the concentration level of the exhaustive electrolysis experiment), one could ask if the anion-transfer process is intra- or intermolecular, that is, whether the NO_3^- ion moves directly from Cu^{II} to the H-bond-donating cavity or is released to the solution and another NO_3^- from the solution moves to the bis-imidazolium compartment. The question is irrelevant for the bulk electrolysis experiment, which is carried out over the course of minutes, a period in which the labile NO_3^- ions continuously exchange from the binding sites to the solution. However, the intramolecular issue may have sense for a CV experiment carried out at a relatively high-potential scan rate. According to the intramolecular hypothesis, the NO_3^- transfer should not result from a jump from one site to the other, but, more realistically, from the folding of the molecular framework of $[\mathbf{1}]^{2+}$ that brings the anion from the metal to the bis-imidazolium cavity. The distance between the centroid of the bis-imidazolium cavity and the metal centre, as evaluated from molecular models, is about 7 Å. Thus, the concentration of the NO_3^- ion, useful for the intramolecular translocation, is given by one molecule over the volume of the sphere whose centre is the centroid of the bis-imidazolium compartment and whose radius is 7 Å ($\approx$1400 Å^3). This corresponds to a 0.84 M concentration, much higher than that of NO_3^- in the bulk solution, under the typical conditions of the electrochemical experiments (10^{-3}–10^{-4} M) and, on statistical bases, points towards the occurrence of a true intramolecular process.

It is disappointing, but curious, that the redox-driven translocation process takes place only with the NO_3^- ion. This results from the unique combination of two properties of nitrate: 1) its moderate coordinating tendency (which does not afford the decomposition of the $[Cu^{I}(\mathbf{1})]^{3+}$ system) and 2) its definite, although not very pronounced, ability to accept H-bonds. In this respect, it is interesting to consider the behaviour of the single-arm system $[\mathbf{3}]^+$. On addition of $[Cu^{I}(MeCN)_4]ClO_4$ to an MeCN solution containing an excess of the single-arm system $[\mathbf{3}]^+$, no colour develops and metal coordination to the bpy fragment does not take place.

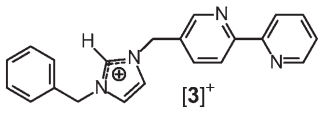

$[\mathbf{3}]^+$

However, if $[Bu_4N]NO_3$ is added to this solution, the brick-red colour of the $[Cu^I(L)_2]^+$ species develops, indicating that metal complexation takes place and requires the additional contribution from the hydrogen-bonding interaction between nitrate and imidazolium subunits. While this feature provides a nice procedure for the colourimetric detection of the elusive nitrate ion (other anions do not have any effect), it also demonstrates the intrinsically poor binding tendencies of the bpy–imidazolium system. Ligands $[\mathbf{1}]^{2+}$ and $[\mathbf{2}]^{2+}$ succeeded in forming relatively stable complexes with Cu^I because their bpy subunits belong to the same framework, thus profiting from the chelate effect.

Conclusion

The redox-driven transfer of an anion between two compartments of different binding tendencies (metal–ligand and hydrogen-bonding interactions) has been described. The investigated systems ($[\mathbf{1}]^{2+}$ and $[\mathbf{2}]^{2+}$) allow the conversion of electrochemical energy into a controlled and repeatable movement and, in this sense, can be considered a further example of a molecular machine.[30] The Cu^{II}/Cu^I couple plays a primary role as it mediates the uptake of electrochemical energy and determines, through the oxidation state of the metal, the location of the anion in one or the other available compartment of the ditopic receptor. This unique feature is related to the fact that the one-electron uptake/release makes the metal cross the border between two realms of very different habits and lifestyles of transition (e.g. d^9) and of post-transition (e.g. d^{10}) metals. It is not accidental that a significant proportion of redox-driven supramolecular machines and motors are based on the Cu^{II}/Cu^I couple within a polypyridine coordinative environment.[31] The system investigated here is able to translocate only the NO_3^- ion, while more ligating anions, such as Cl^- and Br^-, form stable binary complexes with the Cu^I ion, inducing the decomposition of the polypyridine complex. This is an obligatory consequence of the intrinsically low coordinating tendencies of $[\mathbf{1}]^{2+}$ and $[\mathbf{2}]^{2+}$, which results from the electrostatic repulsions between the two imidazolium subunits.

Experimental Section

General procedures and materials: All reagents for syntheses were purchased from Aldrich/Fluka and used without further purification. All reactions were performed under N_2. 5-(Bromomethyl)bipyridine was prepared according to the literature procedure.[32] UV/Vis spectra were recorded on a Varian CARY 100 spectrophotometer, with quartz cuvettes of the appropriate path length (0.1 or 0.01 cm). In any case, the concentration of the chromophore and the optical pathway were adjusted to obtain spectra with $AU \leq 1$. In the titrations with anions, the UV/Vis spectra of the samples were recorded after the addition of aliquots of an alkylammonium salt solution of the envisaged anion ($[Bu_4N]^+$ for Br^-, NO_3^- and NCS^-; $[BnBu_3N]^+$ for Cl^-; Bn: benzyl). All spectrophotometric titration curves were fitted with the HYPERQUAD program.[29] ^1H NMR spectra were obtained on a Bruker Avance 400 spectrometer (400 MHz) operating at 9.37 T. Proton assignments were made on the basis of correlated spectroscopy (COSY) experiments. Electrochemical experiments (CV and controlled-potential coulometry, CPC) were performed with a BAS 100B/W electrochemical workstation. In CV studies (on a solution of $[Bu_4N]ClO_4$ in MeCN (0.1 M)), the working electrode was a platinum microsphere and the counter-electrode a platinum wire. An Ag/AgCl electrode was used as pseudo-reference and was calibrated versus ferrocene as an internal standard. The measured potentials were referred to the Fc^+/Fc couple (425 mV versus SCE, in CH_3CN). CPC experiments were performed on solutions of $[\mathbf{1}]^{2+}$, $Cu^{II}(CF_3SO_3)_2$ and $[Bu_4N]NO_3$ (all 4.00×10^{-3} M), with a platinum gauze as working electrode and a platinum coil as counter-electrode. The counter-electrode compartment was separated from the working compartment by a glass frit. All compartments were filled with a solution of $[Bu_4N]ClO_4$ in MeCN (0.1 M). The reference electrode was an Ag/AgCl electrode calibrated versus Fc^+/Fc through CV experiments prior to the CPC.

Synthesis of $[\mathbf{1}](PF_6)_2$: A mixture of imidazole (1.2 g, 19 mmol) and sodium hydride (0.79 g, 34 mmol) in dry THF (100 mL) was stirred for 15 min at room temperature. 1,4-Di(bromomethyl)benzene (1.26 g, 4.75 mmol) was added to the mixture, which was further stirred overnight at room temperature. Water was then added and THF was rotary evaporated. The water phase was extracted with CH_2Cl_2 (3×70 mL); the collected organic phases were first washed with water (100 mL) and then dried over Na_2SO_4. Filtration and evaporation of the solvent yielded a white solid, which was immediately engaged in the next step. The crude product (0.15 g, 0.63 mmol) was dissolved in dry MeCN (40 mL) and 5-(bromomethyl)bipyridine (0.40 g, 1.60 mmol) was added. The mixture was refluxed for three days, after which a white precipitate appeared. The solution was cooled to room temperature. The white precipitate was isolated by filtration, washed with MeCN and dissolved in the minimum amount of methanol. A saturated aqueous solution of KPF_6 was poured onto the solution, and the resulting solid was collected and washed with water. $[\mathbf{1}](PF_6)_2$ was obtained as a white solid (0.28 g, 52% yield). ^1H NMR (400 MHz, CD_3CN): $\delta=8.70$ (m, 6H; H_a, H_6, $H_{6'}$), 8.52 (d, $J=8.0$ Hz, 2H; H_3), 8.46 (d, $J=8.0$ Hz, 2H; $H_{3'}$), 7.95 (t, $J=7.0$, 8.0 Hz, 2H; $H_{4'}$), 7.90 (dd, $J=2.0$, 8.0 Hz, 2H; H_4), 7.45 (m, 10H; H_α, H_β, H_b, H_c, $H_{5'}$), 5.30 (s, 4H; H_δ), 5.42 ppm (s, 4H; H_γ); ^{13}C NMR (400 MHz, CD_3CN): $\delta=157.1$, 155.4, 149.9, 149.8, 138.0, 137.8, 136.4, 135.1, 129.8, 124.9, 123.5, 123.3, 121.3, 117.8, 52.8, 50.8 ppm; ESI-MS for $C_{36}H_{32}N_8P_2F_{12}$: m/z: 288 $[M-2PF_6]^{2+}$.

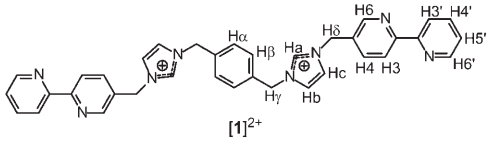

$[\mathbf{1}]^{2+}$

Synthesis of $[\mathbf{2}](PF_6)_2$: The synthesis was performed as previously described for $[\mathbf{1}](PF_6)_2$. 1,3-Di(bromomethyl)benzene (1.26 g, 4.75 mmol) was allowed to react for 12 h with a mixture of imidazole (1.2 g, 19 mmol) and sodium hydride (0.79 g, 34 mmol) in dry THF (100 mL). After treatment with water, the mixture was extracted with CH_2Cl_2 (3×70 mL). The organic phase was washed with water and dried over Na_2SO_4. Evaporation of CH_2Cl_2 gave rise to a sticky white product, which was employed in the next reaction without purification. The crude product (0.15 g, 0.63 mmol) was dissolved in dry MeCN and treated with 5-(bromomethyl)bipyridine (0.40 g, 1.60 mmol). After the mixture was refluxed for three days, the white precipitate was collected, dissolved in methanol and the solution was treated with an aqueous solution of KPF_6.

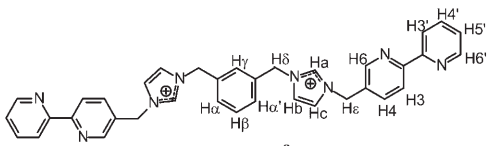

$[\mathbf{2}]^{2+}$

[**2**]$(PF_6)_2$ was obtained as a white solid and collected by filtration under vacuum (0.32 g, 58% yield).

^{1}H NMR (400 MHz, CD_3CN): $\delta = 8.82$ (m, 6H; H_a, H_6, $H_{6'}$), 8.52 (d, $J = 8.0$ Hz, 2H; H_3), 8.48 (d, $J = 8.0$ Hz, 2H; $H_{3'}$), 7.92 (m, 4H; H_4, $H_{4'}$), 7.40 (m, 10H; H_α, $H_{\alpha'}$, H_β, H_γ, H_b, H_c, $H_{5'}$), 5.32 (s, 4H; H_ε), 5.40 ppm (s, 4H; H_δ); ^{13}C NMR (400 MHz, CD_3CN): $\delta = 155.5$, 154.2, 149.9, 148.8, 147.0, 139.2, 138.3, 136.4, 135.0, 130.6, 130.5, 129.9, 129.5, 125.4, 123.4, 121.8, 121.5, 120.8, 119.9, 117.8, 87.5, 83.1, 53.2, 50.7 ppm; ESI-MS for $C_{36}H_{34}N_8P_2F_{12}$: m/z: 288 $[M-2PF_6]^{2+}$.

Synthesis of [3]PF_6: A mixture of imidazole (0.65 g, 10.3 mmol) and sodium hydride (0.43 g, 18.6 mmol) in dry THF (100 mL) was stirred for 15 min at room temperature. 5-(Bromomethyl)bipyridine (1.28 g, 5.1 mmol) in THF (150 mL) was added to the mixture, which was further stirred overnight at room temperature. Water was then added and THF was rotary evaporated. The water phase was extracted with CH_2Cl_2 (3×100 mL); the collected organic phases were first washed with water (100 mL) and then dried over Na_2SO_4. Filtration and evaporation of the solvent yielded an oily product, which was immediately used in the next step. The crude product (0.29 g, 1.23 mmol) was dissolved in $CHCl_3$ (40 mL) and benzyl bromide (175 μL, 1.47 mmol) was added. The mixture was refluxed for three days, then the solvent was removed and the orange residue was dissolved in the minimum amount of water. The obtained solution was treated with saturated NH_4PF_6 until the complete precipitation of [**3**]PF_6 as a light-orange solid (0.23 g, 40% yield).

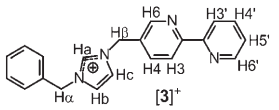

^{1}H NMR (400 MHz, CD_3CN): $\delta = 8.72$ (broad s, 2H; H_6, $H_{6'}$), 8.65 (s, 1H; H_a), 8.52 (d, $J = 8.0$ Hz, 1H; H_3), 8.46 (d, $J = 8.0$ Hz, 1H; $H_{3'}$), 7.95 (t, $J = 7.0$, 8.0 Hz, 1H; $H_{4'}$), 7.90 (dd, $J = 2.0$, 8.0 Hz, 1H; H_4), 7.45 (m, 8H; H_{Bz}, H_b, H_c, $H_{5'}$), 5.32 (s, 2H; H_β), 5.41 ppm (s, 2H; H_α); ESI-MS for $C_{21}H_{19}N_4PF_6$: m/z: 327 $[M]^+$.

Acknowledgements

The financial support of the Italian Ministry of University and Research (PRIN—Dispositivi Supramolecolari; FIRB—Project RBNE019H9K) is gratefully acknowledged.

[1] R. A. Bissell, E. Córdova, A. E. Kaifer, J. F. Stoddart, *Nature* **1994**, *369*, 133–137.
[2] A. Livoreil, C. O. Dietrich-Buchecker, J.-P. Sauvage, *J. Am. Chem. Soc.* **1994**, *116*, 9399–9400.
[3] V. Balzani, A. Credi, M. Ventury, *Molecular Devices and Machines: A Journey Into the Nanoworld*, Wiley-VCH, Weinheim, **2003**.
[4] J.-M. Lehn, *Supramolecular Chemistry: Concepts and Perspectives*, Wiley-VCH, Weinheim, **1995**, pp. 135–138.
[5] L. Zelikovich, J. Libman, A. Shanzer, *Nature* **1995**, *374*, 790–792.
[6] A. Lutz, T. R. Ward, M. Albrecht, *Tetrahedron* **1996**, *52*, 12197–12208.
[7] A. Lutz, T. R. Ward, *Helv. Chim. Acta* **1998**, *81*, 207–218.
[8] C. Canevet, J. Libman, A. Shanzer, *Angew. Chem.* **1996**, *108*, 2842–2845; *Angew. Chem. Int. Ed. Eng.* **1996**, *35*, 2657–2660.
[9] P. Belle, J.-L. Pierre, E. Saint-Aman, *New J. Chem.* **1998**, *22*, 1399–1402.
[10] S. Zahn, J. W. Canary, *Angew. Chem.* **1998**, *110*, 321–323; *Angew. Chem. Int. Ed.* **1998**, *37*, 305–307.
[11] T. R. Ward, A. Lutz, S. P. Parel, J. Ensling, P. Gütlich, P. Buglyó, C. Orvig, *Inorg. Chem.* **1999**, *38*, 5007–5017.
[12] D. Kalny, M. Elhabiri, T. Moav, A. Vaskevich, I. Rubinstein, A. Shanzer, A.-M. Albrecht-Gary, *Chem. Commun.* **2002**, 1426–1427.
[13] V. Amendola, L. Fabbrizzi, C. Mangano, P. Pallavicini, A. Perotti, A. Taglietti, *J. Chem. Soc. Dalton Trans.* **2000**, 185–189.
[14] V. Amendola, L. Fabbrizzi, C. Mangano, P. Pallavicini, *Acc. Chem. Res.* **2001**, *34*, 488–493.
[15] V. Amendola, C. Brusoni, L. Fabbrizzi, C. Mangano, H. Miller, P. Pallavicini, A. Perotti, A. Taglietti, *J. Chem. Soc. Dalton Trans.* **2001**, 3528–3533.
[16] V. Amendola, L. Fabbrizzi, C. Mangano, H. Miller, P. Pallavicini, A. Perotti, A. Taglietti, *Angew. Chem.* **2002**, *114*, 2665–2668; *Angew. Chem. Int. Ed.* **2002**, *41*, 2553–2556.
[17] L. Fabbrizzi, F. Foti, S. Patroni, P. Pallavicini, A. Taglietti, *Angew. Chem.* **2004**, *116*, 5183–5187; *Angew. Chem. Int. Ed.* **2004**, *43*, 5073–5077.
[18] A. Aurora, M. Boiocchi, G. Dacarro, F. Foti, C. Mangano, P. Pallavicini, S. Patroni, A. Taglietti, R. Zanoni, *Chem. Eur. J.* **2006**, *12*, 5535–5546.
[19] L. Fabbrizzi, M. Licchelli, P. Pallavicini, *Acc. Chem. Res.* **1999**, *32*, 846–853.
[20] G. De Santis, L. Fabbrizzi, D. Iacopino, P. Pallavicini, A. Perotti, A. Poggi, *Inorg. Chem.* **1997**, *36*, 827–832.
[21] L. Fabbrizzi, F. Gatti, P. Pallavicini, E. Zambarbieri, *Chem. Eur. J.* **1999**, *5*, 682–690.
[22] a) *Supramolecular Chemistry of Anions* (Eds.: A. Bianchi, K. Bowman-James, E. García-España), Wiley-VCH, New York, **1997**; b) F. P. Schmidtchen, M. Berger, *Chem. Rev.* **1997**, *97*, 1609–1646; c) P. D. Beer, *Acc. Chem. Res.* **1998**, *31*, 71–80; d) P. D. Beer, P. A. Gale, *Angew. Chem.* **2001**, *113*, 502–532; *Angew. Chem. Int. Ed.* **2001**, *40*, 486–516; e) P. A. Gale, *Coord. Chem. Rev.* **2003**, *240*, 1–226, f) R. Martínez-Máòez; F. Sancenón *Chem. Rev.* **2003**, *103*, 4419–4476; g) V. Amendola, D. Esteban-Gomez, L. Fabbrizzi, M. Licchelli, *Acc. Chem. Res.* **2006**, *39*, 343–353; h) V. Amendola, M. Bonizzoni, D. Esteban-Gómez, L. Fabbrizzi, M. Licchelli, F. Sancenón, A. Taglietti, *Coord. Chem. Rev.* **2006**, *250*, 1451–1470; i) J. W. Steed, *Chem. Commun.* **2006**, 2637–2649; j) P. A. Gale, *Acc. Chem. Res.* **2006**, *39*, 465–475.
[23] J. L. Sessler, P. A. Gale, W. S. Cho, *Anion Receptor Chemistry*, (Monographs in Supramolecular Chemistry, Ed.: J. F. Stoddart), Royal Society of Chemistry, Cambridge, **2006**.
[24] J. Yoon, S. K. Kim, N. J. Singh, K. S. Kim, *Chem. Soc. Rev.* **2006**, *35*, 355–360.
[25] A. P. Smith, L. C. Fraser in *Comprehensive Coordination Chemistry II*, Vol. 1 (Eds.: J. A. McCleverty, T. J. Meyer), Elsevier, New York, **2004**, pp. 1–23.
[26] V. Amendola, M. Boiocchi, B. Colasson, L. Fabbrizzi, M.-J. Rodriguez Douton, F. Ugozzoli, *Angew. Chem.* **2006**, *118*, 7074–7078; *Angew. Chem. Int. Ed.* **2006**, *45*, 6920–6924.
[27] Representative examples of X-ray-determined molecular structures of $[Cu^{II}(bpy)_2(X)]^+$ complexes include: X = Cl^-, Br^-, I^-: a) C. O'Sullivan, G. Murphy, B. Murphy, B. Hathaway, *J. Chem. Soc. Dalton Trans.* **1999**, 1835–1844; X = NCS^-: b) A. Sedov, J. Kozisek, M. Kabesova, M. Dunaj-Jurco, J. Gazo, J. Garaj, *Inorg. Chim. Acta* **1983**, *75*, 73; X = NO_3^-: c) P. Y. Zavalij, B. L. Burton, W. E. Jones, Jr., *Acta Crystallogr. C: Cryst. Struct. Commun.* **2002**, *58*, m330.
[28] For structural parameters of the $[Cu^I(bpy)_2]^+$ complex, see: a) H. Nakai, *Bull. Chem. Soc. Jpn.* **1983**, *56*, 1637–1641; b) M. Munakata, S. Kitagawa, A. Asahara, H. Masuda, *Bull. Chem. Soc. Jpn.* **1987**, *60*, 1927–1929.
[29] P. Gans, A. Sabatini, A. Vacca, *Talanta* **1996**, *43*, 1739–1753.
[30] a) V. Balzani, M. Gomez-Lopez, J. F. Stoddart, *Acc. Chem. Res.* **1998**, *31*, 405–414; b) V. Balzani, M. Clemente-León, A. Credi, B. Ferrer, M. Venturi, A. H. Flood, J. F. Stoddart, *Proc. Natl. Acad. Sci. USA* **2006**, *103*, 1178–1183.
[31] a) J.-P. Sauvage, *Acc. Chem. Res.* **1998**, *31*, 611–619; b) J.-P. Collin, C. Dietrich-Buchecker, P. Gavina, M. C. Jimenez-Molero, J.-P. Sauvage, *Acc. Chem. Res.* **2001**, *34*, 477–487.
[32] J. Uenishi, T. Tanaka, K. Nishiwaki, S. Wakabayashi, S. Oae, H. Tsukube *J. Org. Chem.* **1993**, *58*, 4382–4388.

Received: December 22, 2006
Published online: March 15, 2007

